Title

Subtype-Specific MEK-PI3 Kinase Feedback as a Therapeutic Target in Pancreatic Adenocarcinoma

Journal

Molecular Cancer Therapeutics, 12(10)

ISSN

1535-7163

Authors

Mirzoeva, Olga K
Collisson, Eric A
Schaefer, Peter M
et al.

Publication Date

2013-10-01

DOI

10.1158/1535-7163.mct-13-0104

Peer reviewed

Published in final edited form as:
Mol Cancer Ther. 2013 October ; 12(10): 2213–2225. doi:10.1158/1535-7163.MCT-13-0104.

Subtype Specific MEK – PI3 Kinase Feedback as a Therapeutic Target in Pancreatic Adenocarcinoma

Olga K. Mirzoeva[1], **Eric A. Collisson**[2,3], **Peter M. Schaefer**[1,*], **Byron Hann**[3], **Yun K. Hom**[3], **Andrew H. Ko**[2,3], and **W. Michael Korn**[1,2,3,4]

[1]Division of Gastroenterology, Department of Medicine, University of California, San Francisco, CA, USA

[2]Division of Hematology and Oncology, Department of Medicine, University of California, San Francisco, CA, USA

[3]Helen Diller Family Comprehensive Cancer Center, University of California San Francisco, CA

Abstract

Mutations in the KRAS oncogene are dominant features in pancreatic adenocarcinoma (PDA). Since KRAS itself is considered “undruggable”, targeting pathways downstream of KRAS is being explored as a rational therapeutic strategy. We investigated the consequences of MEK inhibition in a large PDA cell line panel. Inhibition of MEK activated PI3 kinase in an EGFR-dependent fashion and combinations of MEK and EGFR inhibitors synergistically induced apoptosis. This combinatorial effect was observed in the epithelial but not mesenchymal subtype of PDA. RNA expression analysis revealed predictors of susceptibility to the combination, including E-cadherin, HER3, and the miR200-family of micro-RNAs, while expression of the transcription factor ZEB1 was associated with resistance to the drug combination. Knock-down of HER3 in epithelial-type and ZEB1 in mesenchymal-type PDA cell lines resulted in sensitization to the combination of MEK and EGFR inhibitors. Thus, our findings suggest a new, subtype-specific and personalized therapeutic strategy for pancreatic cancer.

Keywords

MEK; EGFR; HER3; PI3 kinase; pancreatic adenocarcinoma; cancer signal transduction; epithelial-to-mesenchymal transition

Introduction

The prognosis for patients with pancreatic ductal adenocarcinoma (PDA) remains dismal despite recent modest improvements resulting from optimized use of systemic chemotherapy (1, 2). Effective therapeutic targeting of key pathways involved in the pathogenesis of this disease could lead to substantial improvements in outcome. The presence of mutations in the KRAS oncogene in more than 90% of PDAs has long been documented (3). Genetically engineered mouse models of pancreatic cancer have proved the crucial role of this mutation for tumorigenesis and tumor maintenance (4). Activating mutations in KRAS result in constitutive signaling through effector pathways (5). Indeed, presence of phosphorylated

[4]Corresponding author: W. Michael Korn, M.D. Associate Professor of Medicine In Residence, UCSF Divisions of Gastroenterology and Hematology/Oncology, Helen Diller Family Comprehensive Cancer Center, 2340 Sutter St., Box 1387, San Francisco, CA 94115, USA, Phone office: (415) 502 2844, Phone lab: (415) 476 0137, FAX: (415) 502 4787, Michael.Korn@ucsf.edu.
[*]Current address: Peter M. Schaefer, Weill Cornell Medical College, New York, NY, 1300 York Ave., New York, NY 10065

Conflict of interest statement: The authors have no conflicts of interest to disclose.

ERK and AKT in PDA is associated with poor prognosis (6). Since mutant KRAS is considered “undruggable” (7) pathways up- and down-stream of RAS have emerged as attractive therapeutic targets (8). However, clinical results with specific inhibitors of these pathways have been disappointing. For example, the EGFR inhibitor erlotinib was approved by the U.S. Food and Drug Administration for use in PDA in combination with gemcitabine despite only a very modest improvement in median overall survival (9). Available efficacy data on single agent activity of inhibitors of MEK and PI3K have also demonstrated limited tumor activity (10, 11). Recent data from our institution demonstrate the existence of molecularly defined sub-types of PDA with differential sensitivity to conventional chemotherapy (12). Thus, inefficacy of targeted therapies for this disease might be a consequence of failure to understand the subtype-dependent complexities of molecular networks associated with the therapeutic target. Signaling in response to treatment with targeted agents has been demonstrated to result in feedback activation of anti-apoptotic and other important cellular pathways. For example, S6K1-mediated feedback activation of AKT and eIF4E in response to pharmacological inhibition of mTOR resulting in activation of cell survival pathways has been well documented (13, 14). Similarly, we discovered a novel, EGFR-dependent, feedback loop resulting in PI3K activation in response to inhibition of MEK (15).

The relevance of this mechanism is highlighted by our finding that interruption of this feedback, e.g. by combining MEK inhibitors with inhibitors of EGFR or PI3K, results in synergistic induction of cell cycle arrest or apoptosis in breast cancer (15, 16) models. In addition, Diep *et al* reported similar findings exclusively in PDA with wild-type KRAS (17). Herein we examine both the frequency and determinants of this feedback loop in addition to examining the consequences of interrupting the feedback loop in cell line and *in vivo* models of pancreatic cancer. We identify synergistic interactions between targeted agents within this feedback loop and identify pretreatment molecular predictors of this synergy within specific PDA subtypes. These studies will further inform sensitivity enrichment strategies with MEK / EGFR inhibitor combinations in this disease.

Materials and Methods

Reagents

The following reagents were used: EGF (Millipore), CI1040 (PD 184352) was from Tocris, PD0325901 and Erlotinib were from Selleck. All drugs were diluted in DMSO. The following antibodies were from Cell Signaling Technology: p-AKT (S473), total AKT, p-EGFR (Y1068), p-HER3 (Y1197, Y1289), total HER3, p-PRAS40 (T246), p-GSK3 (S21/9), p-ERK (T202/Y204), beta-actin antibody was from Sigma, ZEB1 (H-102) and E-cadherin (#sc-7870) antibody were from Santa Cruz. Protease inhibitors cocktail set III and phosphatase inhibitor cocktail set II were from EMD Millipore. Structures of Erlotinib, CI1040, PD0325901 are presented in Supplemental Figure 1.

Cell culture

Pancreatic cancer cell lines used in this study were described previously (12, 18, 19). MiaPaCa-2, Panc1, CFPAC-1, HPAF-II, Capan-2, Hs766T, and BxPC-3 cell lines were provided by Dr. Paul Kirschmeier (Schering Plough Research Institute). SW1990, Panc2.03, Panc8.13, and Su86.86 cell lines were purchased from American Type Culture Collection. Panc2.13, Panc3.27, Panc5.04, Panc6.03, and Panc10.05 were provided by Dr. Elizabeth Jaffee (Johns Hopkins University, Baltimore, MD). Colo357 was provided by Dr. Lance Tibbetts, (Brown University, Providence). Panc8.13, YAPC were from J. Settleman, (Massachusetts General Hospital). Suit2, HcG25, Capan-1, and T3M4 were from S.K. Batra (Univ of Nebraska). HupT3, HPAC, DanG, PA-TU8902, PA-TU8988S, PA-TU8988T and

ASPC-1 were from Lynda Chin, (MD Anderson). All cell lines were genotyped by Affymetrix SNP6.0 for definitive future disambiguation of provenance. No additional authentication was done by the authors. All cells were cultured in high glucose DMEM supplemented with 10% FBS (US origin, Valley Biomedical). All PDAC cell lines used in this study had activating KRAS mutations, except one – BxPC3, which harbors wild-type KRAS. RAS mutational status was verified by sequencing at UCSF Genomics Core Facility.

Cell growth inhibition assays—Cells were plated in 96 well plates at the density from 3000 to 12000/well depending on the cell line so they are in logarithmic growth at the time of assay. Cells were allowed to attach overnight before being exposed to the drugs for 72 h. Increasing doses of each drug were added in triplicate wells. The final DMSO concentration was 0.2% or less. Cell viability was determined using the CellTiter-Glo (CTG) assay (Promega, Madison, WI). Drug combination studies were designed according to Chou and Talalay (20). Combined drugs were used at fixed molar ratios. Equitoxic drug doses that produced approximately 50% of growth inhibition in single-agent experiments were chosen to determine an appropriate fixed molar ratio of two combined drugs. For most of the cell lines IC50 was not reached with one or both single agents, therefore the Calcusyn software (Biosoft, Ferguson, MO), commonly used for drug combination studies, was not applicable. The enhancement effect was designated as potentiation when the IC50 from the drug combination treatment was at least 3 fold lower than the lowest IC50 of the single agent.

Apoptosis analysis

Cells were treated with drugs 24 hours after plating and harvested for apoptosis assay at 3 days after drug treatment. Apoptosis was measured in live cells by Annexin V- FITC and propidium iodide (PI) labeling using Apoptosis Detection Kit I (BD Pharmingen) and quantified by Flow Cytometry (FACS Calibur, BD) with FlowJo software. The experiments were done in duplicates and at least 40,000 cells were acquired from every sample for each duplicate. The results were reproduced in three independent experiments.

siRNA transfection

Cells were plated at 20×10^4/ml in 6 well plates and transfected with siRNAs using reverse-transfection protocol with 20nM siRNA and 2.5ul RNAiMax transfection reagent (Invitrogen). 48h after transfection the cells were trypsinized and replated at a required density for the specific assay of drug sensitivity (cell viability or apoptosis.) Drug treatment was started 72h post-transfection (24h post replating). 72h after drug treatment cells were analysed for apoptosis or for cell viability. The following siRNAs were used in this work: non-targeting smartpool siRNA (ON-TARGETplus, Dharmacon #D-001810-10-05), HER3-targeting smartpool siRNA (ON-TARGETplus, Dharmacon #L003127-00-0005). For ZEB1 siRNA experiments we used two negative controls: Ctrl NT, siControl ON-TARGETplus Non-targeting siRNA #1 (Dharmacon); Ctrl FF, firefly luciferase-targeting siRNA. ZEB1 siRNA #1: S/AS 5’-CAGUGAAAGAGAAGGGAAUUU-3’/5’-AUUCCCUUCUCUUUCACUGUU-3’ ZEB1; siRNA #2: S/AS 5’-AACUGAACCUGUGGAUUAUUU-3’/5’-AUAAUCCACAGGUUCAGUUUU-3’.

Preparation of protein lysates and Western blot analysis

The cells were treated with drugs either in low serum or in full serum conditions as indicated in the figures. For the low serum conditions, cells were washed in medium containing 0.1% FBS 24 h after plating and incubated for 24h in this medium. Drugs or DMSO (control) were added followed by addition of EGF at a final dose of 10 ng/ml 30 min later. Cells were harvested at 4 h post EGF stimulation. For full serum conditions, cells were grown in their established growth medium (DMEM with 10% FBS), at 48h after plating were treated with

the drugs and harvested at 4h post drug exposure. Protein lysates were prepared from cells at 70%–90% confluency. The cells were washed in ice-cold PBS, and then extracted in RIPA lysis buffer (Boston Bioproducts) containing protease and phosphatase inhibitor cocktails. The lysates were clarified by centrifugation at 13000 rpm for 10 minutes on ice and frozen at −80°C. Protein concentrations were determined using the BCA protein assay kit (Pierce Biotechnology, Rockford, IL). 20 μg of protein extract per lane was electrophoresed, transferred to Nitrocellulose membranes (BioRad), and probed with specific antisera using standard techniques. Bound antibodies on immunoblots were detected and quantitated by fluorescent imaging (Odyssey imager, Li-COR).

miRNA expression

In order to analyze whether miRNA were differentially expressed in cell lines sensitive or resistant to a combination of EGFRi/MEKi we analysed miRNA expression in 6 sensitive and 6 resistant cell lines. Total RNA was isolated using mirVana kit (Ambion). miRNA assays were performed with 100ng total RNA by Nanostring Technologies (Seattle, WA) based on nCounter Analysis System utilizing digital color-coded barcode technology, as well as by HTG Molecular Inc (Tucson, AZ), using qNPA technology. Out of 733 miRNA screened by Nanostring Tech, 8 miRNAs were highly expressed in sensitive but not in resistant cell lines. Data are presented as direct counts proportional to miRNA expression in each cell line. HTG Molecular assay showed consistent results with the same miRNAs significantly higher expressed in sensitive cell lines.

In vivo xenograft tumor studies

Female 7 - 9 week old Nu/Nu mice (Harlan, FoxN1/nude) were inoculated *s.c.* with 10^7 HPAF-II cells. Mice were monitored according to the protocol approved by the University of California, San Francisco Institutional Animal Care and Use Committee. When tumors reached about 100 mm^3, mice were randomly assigned to one of four treatment groups: vehicle control, Erlotinib 35 mg/kg, PD0325901 7.5 mg/kg, or the drug combination. The drugs were administered by oral gavage once a day 5 times per week. Each treatment regimen was tested in cohorts of eight mice and the dosing was continued for 34 days. Tumor sizes were measured twice weekly in two dimensions using a caliper, tumor size (mm^3) was calculated as (length × $width^2$) / 2. The doses for drug treatments were chosen as MTD according to the preceding toxicity study in mice bearing HPAF-II xenografts. Animals were monitored for the absence of drug toxicity by measuring body weight twice weekly and monitoring overall activity. To assess for target inhibition, 2 mice from each treatment group were sacrificed at day 3 of treatment, 3 h post dosing. Tumors were excised and protein lysates prepared and subjected to Western blot analysis as described above for cell lines.

Statistical analysis

Statistical analysis was performed using Graph Pad Prism software. An unpaired two-tailed t test was used to determine the significance of change in levels of cell viability and apoptosis between different treatment groups. Data are expressed as mean +/- standard deviation. Statistical analysis to compare tumor sizes in xenograft-bearing mice was done with ANOVA with Bonferroni posttests. P values of <0.05 were considered significant.

Correlation analysis of drug sensitivity

mRNA expression data of PDA cell lines panel were described previously (12). The data were normalized by RMA method. Low performing probesets (those with intensity values below a threshold across all samples, the threshold was taken to be the global lowest 25th percentile of intensity values) were excluded from analysis. Differential gene expression for

dichotomous EGFRi + MEKi sensitivity were obtained from moderated t-statistics using the limma package (21) in Bioconductor (22). q-values (23) were calculated to control the false discovery rate and q-values less than 0.01 were considered significant. The expression data was also classified to predict EGFRi + MEKi sensitivity (sensitive or not) by applying nearest shrunken centroid classification using Pam (24) with ten-fold cross-validation and obtaining the top genes with low misclassification error. We obtained the list of 263 and 29 predictors of sensitivity and resistance, respectively. All calculations were performed using the R language (25).

Results

MEK inhibition results in negative feedback activation of PI3 kinase, mediated by the EGF receptor

In our previous work, using models of triple-negative breast cancer, we demonstrated that MEK inhibition induces feedback activation of PI3K mediated by the EGF receptor (15). To investigate whether pathway interactions occur in pancreatic cancer, we treated KRAS mutant (HPAF-II and Panc 10.05) and KRAS-wt (BxPC-3) PDAC cell lines with the MEK inhibitor CI1040, the EGFR inhibitor erlotinib, and their combination at low serum conditions (cell culture medium containing 0.1% fetal bovine serum) in the presence of EGF. As expected, a strong reduction in phosphorylated ERK levels in response to MEK inhibitor treatment was observed (Fig. 1A). However, MEK inhibition led to enhanced phosphorylation of EGFR and activation of the PI3 kinase pathway, as determined by markedly enhanced protein levels of phosphorylated AKT (pS473), PRAS40 (pT246) and GSK3α/β (pS21/9). MEK inhibitor induced activation of AKT was fully abolished by the EGFR inhibitor erlotinib (Fig. 1A). Thus, a negative regulatory feedback loop between MEK and the PI3 kinase pathway is operative in PDA cells and depends on activation of the EGF receptor.

Interruption of MEK-PI3K feedback results in synergistic inhibition of cell viability and induction of apoptosis in PDA cell lines and mouse xenograft tumors

Since MEK inhibition resulted in feedback activation of the EGFR pathway in PDA cell lines, we asked whether a combination of MEK with EGFR inhibitors would elicit synergistic effects on cell survival in PDA cell lines. Indeed, combination of the MEK inhibitors CI1040 or PD0325901 with the EGFR inhibitor erlotinib resulted in synergistic cell growth inhibition in PDA cell lines harboring wild-type (BxPC-3) or mutant KRAS (HPAF-II) (Fig. 1B). This synergistic effect on cell growth was due to highly increased rate of apoptosis as determined by FACS analysis of annexin V/PI positive cells (Fig. 1C). To test whether the combination of MEK and EGFR inhibitors induced enhanced tumor growth inhibition in vivo, we generated subcutaneous xenograft tumors using the human PDA cell line HPAF-II. Tumors were grown to a size of approximately 100 mm^3 and mice were treated with the specific, orally bioavailable MEK inhibitor PD0325901 and erlotinib, either as single agents or in combination, for up to 34 days by oral gavage.

At daily doses of 35 mg/kg of erlotinib and 7.5 mg/kg of PD0325901, an additive effect of both drugs was observed (Fig. 1D). The combination of both drugs administered at higher doses (50 mg/kg of erlotinib and 12.5 mg/kg of PD0325901) resulted in strong synergistic induction of tumor shrinkage. However, increased toxicity was observed at this dose level and the study had to be stopped after 18 days of treatment. Western blot analysis of tumors confirmed inhibition of p-ERK by PD0325901 and p-EGFR by Erlotinib (Fig.1E). The feedback of MEKi-induced activation of p-EGFR, p-AKT, p-PRAS40 and p-GSK3 was also evident *in vivo*, similar to *in vitro* observations in cell lines. However, in contrast to *in vitro*

effect, combination of erlotinib and PD0325901 did not result in complete p-AKT and p-EGFR inhibition *in vivo*, suggesting that additional pathway inputs are operational.

Since molecular profiling of clinical PDA samples from our institution revealed up to three different subtypes of the disease (12), we set out to assess possible subtype-dependent differences between PDA cell lines with respect to their response to the MEK/EGFRi combination. We treated a panel of 29 pancreatic cancer cell lines with increasing concentrations of PD0325901 and the erlotinib. Compounds were administered as single agents or in combination at fixed molar ratios. Since the cell sensitivity to PD0325901 varied greatly, we did the assay in the dose range 0.01 – 1uM, for the combination study at fixed molar ratio we selected the dose which was close to IC50. For each cell line the experiments were done 3 – 4 times at different dose ratios to ensure consistency in response pattern and IC50s. Fig. 2A demonstrates representative examples of four different response patterns; the complete dataset of all cell lines responses is presented in Suppl. figure 2. In 11 cell lines single drug treatment had only limited effects on cell viability, but treatment with the drug combination resulted in strong inhibition of cell viability and apparent cell killing, indicating potentiation of activity of one or both drugs (e.g. Panc3.27; Fig. 2A). In 12 cell lines, the potentiation effect was moderate (e.g. Panc10.05; Fig. 2A). In three cell lines, cell viability was only inhibited by the MEK inhibitor and its combination with EGFR inhibitor had no additional effect (e.g. MiaPaCa-2 cells; Fig. 2A). Lastly, three cell lines were resistant to both inhibitors as single agents and to their combination (e.g. Panc2.13; Fig. 2A). The IC50 was calculated for each drug and for their combination using the GraphPad Prism software. If the combined IC50 was at least 7 fold lower (such as for Panc3.27) or 3-6 fold lower (such as for Panc10.05) compared to the lowest IC50 of the single agent, the response was classified as strong synergy/potentiation or as moderate potentiation, respectively. When the combined IC50 was less than 3 fold different than the lowest IC50 of a single drug, the response was classified as “no combinatorial effect” (such as for MiaPaCa-2 or Panc2.13).

In summary, these data clearly demonstrate that the combination of MEK and EGFR inhibitors results in strongly enhanced inhibition of cell and tumor growth. While these effects are independent of the KRAS mutation status there was marked heterogeneity in cell line responses to treatment with the drug combination.

RNA profiling of PDA cell lines reveals genes predictive of synergistic response to the MEK/EGFR inhibitor combination

To elucidate molecular determinants associated with the different response patterns to treatment with the combination of MEK and EGFR inhibitors, we generated mRNA expression profiles for all cell lines in our panel. Correlation analysis between gene expression and drug responses identified probes that were significantly ($q < 0.01$, and difference in expression >2-fold) correlated with cellular sensitivity (263 probes) or resistance (29 probes) to the combination of MEK and EGFR inhibitors in our PDA cell line panel. The complete list of sensitivity and resistance predictors is presented in Supplementary Table 1. Figure 2B illustrates a short list of 32 probes associated with sensitivity ($q < 0.00001$) and 10 probes associated with resistance ($q < 0.01$) which demonstrate a difference in mRNA expression level of greater than 2.5 fold (Fold Change, FC > 2.5). Cell lines were hierarchically clustered according to their expression of response predictors. This analysis revealed that genes known to be markers of epithelial phenotype were highly expressed in the sensitive cell lines, including *CDH1* ($q = 10^{-12}$), *ST14* ($q = 3 \times 10^{-9}$), *KRT7* ($q = 7 \times 10^{-9}$), *KRT19* ($q = 6 \times 10^{-6}$), In contrast, all six resistant cell lines displayed low expression of these genes but demonstrated high levels of *ZEB1* ($q = 0.001$) expression, in agreement with their mesenchymal phenotype. Almost all moderately responsive cell lines clustered to the interface between the sensitive and resistant cell line

clusters (Fig. 2B). In contrast to data from human primary PDAs, there was no apparent acinar subtype (characterized by expression of chymotrypsin-like elastase family members, and regenerating islet-derived genes, among others (12)).

Three genes (*FOXQ1, HER3*, and *ELF3*) identified by us as associated with sensitivity were part of the gene set characterizing the epithelial (classical) subtype of primary human PDAs (12), representing significant overrepresentation ($p<0.0004$; Fisher's exact test). These findings indicate that clinically relevant subtypes of PDA respond differently to the combination of MEK/EGFR inhibition. This has implications for further understanding of underlying molecular mechanisms as well as for patient selection strategies in future trials.

Feedback activation of the PI3K pathway resulting from MEK inhibition in PDA subtypes

We next asked whether the differences in drug sensitivity between epithelial and mesenchymal subtypes were reflected in differential behavior of signal transduction pathways following MEK inhibition. In all cell lines, inhibition of MEK with CI1040 resulted consistently in inhibition of phosphorylation of its effector: ERK. However, in the epithelial-type PDA lines HPAF-II and Panc10.05, increases of phosphorylated AKT levels were detected in cells grown in medium containing 10% FBS following treatment with CI1040 (Fig. 3), although this effect was less evident compared to low serum conditions with EGF stimulation. In epithelial-type cell lines pAKT was strongly inhibited by erlotinib treatment and completely suppressed by its combination with CI1040. In contrast, the mesenchymal-type PDAC lines showed no induction of pAKT following MEK inhibition. In these cells, high basal levels of pAKT remained unchanged following treatment with single inhibitors and their combination. Thus, these data indicate that there are differences in RTK signal transduction between epithelial and mesenchymal-type pancreatic cancer cells which are consistent with differential responses to MEK and EGFR inhibitors and their combination.

Inhibition of HER3 enhances effects of MEK inhibition in epithelial-type PDA

The receptor tyrosine kinase HER3 (*ERBB3*) was found to be among the genes significantly associated with the sensitivity of PDA cell lines to MEKi/EGFRi combination. Since HER3 is well known to mediate signals from EGFR and HER2 to PI3 kinase, we ascertained whether feedback activation of EGFR following MEK inhibition resulted in HER3 activation. As shown in Figure 3, this was indeed the case as we observed a clear increase in HER3 phosphorylation at Y1197 and Y1289 in response to treatment with CI1040 in epithelial-type cells. In contrast, mesenchymal type cells, as expected, had low basal expression of HER3, and did not show any increase in HER3 phosphorylation in response to MEK inhibition.

The phosphorylation of HER3 of both Y1197 and Y1289 was also induced *in vivo*, in tumor xenograft tissues of mice treated with MEK inhibitor (Fig. 1E). Taken together, these findings suggested that HER3 might represent a meaningful therapeutic target in combination with MEK inhibitors specific to epithelial subtype PDA. To explore this possibility, we utilized siRNAs targeting HER3 that effectively reduced HER3 protein levels when transfected into various PDA lines. As determined by quantitative Western blot analysis, HER3 expression decreased 2-5 fold at 72h post-transfection with siRNA (pool of 4), depending on cell line (Fig. 4A). Mesenchymal cell lines, such as Panc2.13, had very low basal expression of HER3 protein that was not changed after siRNA knock-down.

In agreement with our hypothesis, epithelial PDA cell lines in which HER3 had been knocked-down showed significantly higher rates of apoptosis in response to single inhibitors or to MEK/EGFR combined inhibition (Fig. 4B). The drug-induced apoptosis rate in cells

treated with triple HER3/MEK/EGFR suppression reached 50 – 80% depending on the cell line. Knockdown of HER3 in addition to EGFR inhibition might increase apoptosis induction due to a greater degree of inhibition of signal flow from EGFR to PI3 kinase. Indeed, we observed residual phosphorylation of HER3 following treatment of cells with erlotinib (Figure 3). Furthermore, signals from additional receptor-tyrosine kinases might contribute to this phenomenon. Mesenchymal cell lines (such as Panc2.13), characterized by low levels of HER3, also displayed apoptosis increase, although the overall apoptotic rate was below 10% (Fig.4B). Therefore, knockdown of HER3 did not sensitize mesenchymal cells to the combination of MEK and EGFR inhibitors. These data suggest that combinations of MEK and EGFR as well HER3 inhibitors may be particularly effective in epithelial subtype of PDA cells.

miRNA expression of miR200 family is significantly downregulated in resistant PDA cells

In cancer cells, epithelial and mesenchymal subtypes are maintained through molecular circuits including transcription factors, such as ZEB1, SIP1, SNAIL, and SLUG and micro-RNAs, in particular those belonging to the mir200 family. We therefore assessed expression of miRNAs using commercially available technology provided by Nanostring Technologies (Seattle, WA), based on their nCounter Analysis System with digital color-coded barcode technology. We selected 6 sensitive and 6 resistant cell lines based on their response to the PD0325901/erlotinib combination and analyzed global expression of their miRNAs (733 miRNAs in total). We found that all five members of the microRNA-200 family (miR-200a, miR-200b, miR-200c, miR-141 and miR-429) and in addition, miR-155, -139-5p, and 135b were markedly upregulated in sensitive, but almost not expressed in resistant cell lines (Fig. 5). We compared these results to the data obtained by a different technology available through HTG Molecular (Tucson, AZ) using quantitative nuclease protection assay (qNPA) screening of 1250 miRNAs, and obtained very similar results (data not shown). In addition, we validated miR-200 family expression levels by quantitative PCR performed on total Trizol-isolated RNA. Since miR200 family is known to be crucially involved in regulating epithelial-to-mesenchymal transition (EMT) (26, 27), our findings support the notion that molecular programs regulating differentiation status of PDA cells determine susceptibility to combinations of MEK and EGFR inhibitors.

Suppression of ZEB1 results in sensitization to MEK/EGFR inhibitor combination

Our analysis of molecular predictors of response to the MEK/EGFR inhibitor combination clearly demonstrated that epithelial features significantly correlated with sensitivity. High E-cadherin expression was found to be the strongest predictor of sensitivity, whereas ZEB1 expression was found to be significant predictor of resistance to the MEK/EGFR inhibitor combination. ZEB1 is a well-characterized repressor of E-cadherin transcription and promoter of EMT (28). ZEB1 also regulates and is regulated by, as part of a double-negative feedback loop, expression of micro-RNAs of the miR200 family (29). In agreement with this, we found that miR200 family levels were downregulated in resistant cells lines. Therefore, we asked whether knock-down of ZEB1 would result in mesenchymal-to-epithelial transition and in sensitization to the inhibitor combination. We utilized two ZEB1 siRNAs that we optimized and validated previously (30) and compared their effect with two controls: non-targeting and Firefly luciferase-targeting siRNAs. Indeed, knock down of ZEB1 in mesenchymal-type PDA cells (Panc2.13, HS766T, and PA-TU8988T) resulted in more than 90% inhibition of ZEB1 protein expression (Fig. 6A). Following knock-down, noticeable changes in cell morphology resulting in less predominant spindle-cell phenotype were observed (data not shown). This was accompanied by a marked up-regulation of E-cadherin protein expression (Fig.6A), and activation of pAKT and pHER3 above the background levels in mesenchymal cells (Suppl. Fig. 3). In contrast, knock-down of ZEB1 in epithelial cells (which have very low ZEB1 expression) had no effect on E-cadherin

levels (Panc10.05 cells, Fig. 6A, HPAF-II cells, Suppl. Fig. 3). In agreement with these biochemical findings, knockdown of ZEB1 in mesenchymal-type PDA cells resulted in moderate increases in apoptosis rates in cell treated with single-agent erlotinib or CI1040 while a significant increase in apoptosis rates was observed in cells treated with the combination of both (Fig. 6B). These phenomena were strongly contrasted by observations in epithelial-type PDA cells that did not demonstrate differences in apoptosis rates with or without knockdown of ZEB1.

Discussion

The RAS oncogene, which is mutated in the vast majority of pancreatic cancers (31), has resisted direct therapeutic targeting with small-molecule inhibitors. Thus, inhibition of RAS effector pathways such as the RAF-MEK-ERK pathway represents a rational alternative strategy. However, initial clinical experience with second-generation MEK inhibitors has been disappointing, with the exception of BRAF-mutant melanoma (31). Previously, we demonstrated that MEK inhibition leads to EGFR-dependent feedback activation of the PI3K pathway in basal-type breast cancer, which utilizes the RAF-MEK-ERK pathway preferentially (15). Here, we demonstrate that MEK inhibition in pancreatic cancer also leads to EGFR-mediated PI3K activation and, as a result, profound sensitivity to combinations of MEK and EGFR inhibitors in PDA cell line models. These findings occur independent of the KRAS mutation status, in contrast to observations published by others (17). Our study expands on the published literature substantially as we identify phenotypic differences as crucial predictors of sensitivity to the drug combination, thus setting the stage for patient selection strategies in future trials of this combination.

The KRAS oncogene is predicted to result in consistent activation of the RAF-MEK-ERK signal transduction cascade. In agreement with this hypothesis, expression of mutant $BRAF^{V600E}$ but not $PIK3CA^{H1047R}$ is sufficient to induce PanIN formation in conjunction with mutant $p53^{R270H}$ in transgenic mouse models (32). In addition, studies of the effects of MEK inhibitors in pancreatic cancer cell lines demonstrate the dependence of these cells on the RAF-MEK-ERK pathway for their proliferation (33). Consistent with these data, expression levels of phosphorylated ERK in pancreatectomy specimens was found to be correlated with poor survival (6). Thus, targeting this pathway therapeutically and understanding mechanisms of *de novo* resistance is of particular biological and clinical significance.

Cellular signal transduction networks are complex functional units that are regulated in their activity by feedback and feed-forward mechanisms resulting in frequently non-intuitive network behaviors in response to targeted inhibitors. Increasing evidence suggests that feedback mechanisms indeed confer *de novo* resistance to inhibitors of the broader receptor-tyrosine kinase signal transduction network (reviewed in: (34)). For example, upregulation of the receptor-tyrosine kinase HER3 contributes to resistance to AKT inhibitors (35) while feedback activation of PI3 kinase mediates resistance to mTOR inhibitors (36). Our current study expands on these findings by demonstrating that MEK-dependent feedback activation occurs despite presence of KRAS mutations and highlights a role of HER3 in mediating PI3 kinase activation in this context. HER3 is a kinase-deficient member of the HER kinase family containing six tyrosines in its intracellular domain that, when phosphorylated, mediate high-affinity binding to the p85 subunit of PI3 kinase (37). In our experiments, inhibition of MEK resulted in increased phosphorylation of HER3. Underscoring the functional relevance of this effect, siRNA-mediated inhibition of HER3 in combination with MEK inhibitors resulted in significantly increased apoptosis rates, in particular in epithelial type PDA cell lines. Addition of erlotinib further enhanced this effect. Our findings are consistent with previous studies demonstrating that persistence of HER3 activation in cells

treated with EGFR or HER2 kinase inhibitors is a crucial factor in mediating resistance to these inhibitors (38). Thus, combinations of compounds targeting MEK and HER3 with or without EGFR inhibitors might have substantial therapeutic potential.

Recent analyses of molecular profiles of human pancreatic cancers revealed the existence of at least three distinct subtypes: classical (epithelial-like), quasimesenchymal, and exocrine-like (12). Of those, epithelial-like and quasimesenchymal subtypes are present in cell line models of pancreatic cancer while the exocrine-like subtype is not represented in this setting. These subtypes are strongly associated with differential susceptibility to therapeutics. For example, the quasimeschymal subtype lacks responsiveness to erlotinib (12). Here we expand on this theme by demonstrating that synergistically enhanced cell killing by the combination of MEK and EGFR inhibitors is restricted to cell lines with epithelial characteristics as determined by mRNA and miRNA profiling. We identified subsets of genes and miRNAs (in particular the mir200 family) that are strongly predictive of synergistic cell killing activity of the drug combination. Strong evidence suggests that the miR-200 family plays an important role in mediating epithelial versus mesenchymal differentiation in tumor cells by targeting the repressors of *CDH1,* in particular ZEB1 and ZEB2 (Sip1) (26, 27). Interestingly, an inverse relationship between ZEB proteins and miR200 family has been found, revealing a dual-negative feedback loop regulating and maintaining the differentiation state of tumor cells (26, 29). Previously, it was demonstrated that mesenchymal differentiation of tumor cells promotes resistance to EGFR inhibitors (39, 40). In agreement with these findings, miRNA signature predictive of sensitivity to EGFR inhibitors is strongly enriched for miRNAs involved in maintaining epithelial differentiation (41). Here, we demonstrate that induction of mesenchymal-to-epithelial transition by inhibition of ZEB1 expression results in marked sensitization to the combination of MEK and EGFR inhibitors. Re-expression of *CDH1* has been demonstrated before to restore sensitivity to EGFR inhibitors (42). Thus, it is conceivable that reversal of EMT by repression of ZEB1 restores molecular circuits critical for EGFR activation of anti-apoptotic pathways following MEK inhibition. The results of these studies hold significant clinical relevance in the treatment of pancreatic cancer, which continues to be a devastating disease for the majority of patients. Based on our findings, we have completed a clinical phase-II trial that tested the efficacy of a combination of the MEK inhibitor AZD6244 in combination with erlotinib in patients with advanced, gemcitabine-refractory pancreatic cancer (Protocol ID #NCT01222689 in clinicaltrials.gov). Tissue samples obtained from patients before enrollment into the study will allow us to further validate candidate predictive markers identified in the cell line panel. Future studies will employ patient selection strategies based on the results of these studies. In addition, based on our findings, exploration of novel combinations involving MEK and HER3 inhibitors, as well as agents capable of reversing EMT, is warranted.

Supplementary Material

Refer to Web version on PubMed Central for supplementary material.

Acknowledgments

We acknowledge the work of the UCSF Preclinical Therapeutics Core, UCSF Genomics and Cell Analysis Core. We are thankful to Ritu Roy for statistical support and David Ginzinger for technical support.

Grant Support: This work was supported in part by NIH grants U54 CA11297 (W.M. Korn), and K08 CA137153 (E.A. Collisson), P30 CA82103 (Comprehensive Cancer Center Support Grant, F. McCormick), grant 12-20-25 COLL from the Pancreatic Cancer Action Network (E.A. Collisson), as well as grants from the UCSF Pancreatic Cancer Program (W.M. Korn), and the UCSF School of Medicine (W.M. Korn).

References

1. Conroy T, Desseigne F, Ychou M, Bouche O, Guimbaud R, Becouarn Y, et al. FOLFIRINOX versus gemcitabine for metastatic pancreatic cancer. The New England journal of medicine. 2011; 364:1817–25. [PubMed: 21561347]
2. Von Hoff DD, Ramanathan RK, Borad MJ, Laheru DA, Smith LS, Wood TE, et al. Gemcitabine plus nab-paclitaxel is an active regimen in patients with advanced pancreatic cancer: a phase I/II trial. Journal of clinical oncology : official journal of the American Society of Clinical Oncology. 2011; 29:4548–54. [PubMed: 21969517]
3. Almoguera C, Shibata D, Forrester K, Martin J, Arnheim N, Perucho M. Most human carcinomas of the exocrine pancreas contain mutant c-K-ras genes. Cell. 1988; 53:549–54. [PubMed: 2453289]
4. Hingorani SR, Wang L, Multani AS, Combs C, Deramaudt TB, Hruban RH, et al. Trp53R172H and KrasG12D cooperate to promote chromosomal instability and widely metastatic pancreatic ductal adenocarcinoma in mice. Cancer cell. 2005; 7:469–83. [PubMed: 15894267]
5. Downward J. Targeting RAS signalling pathways in cancer therapy. Nat Rev Cancer. 2003; 3:11–22. [PubMed: 12509763]
6. Chadha KS, Khoury T, Yu J, Black JD, Gibbs JF, Kuvshinoff BW, et al. Activated Akt and Erk expression and survival after surgery in pancreatic carcinoma. Annals of surgical oncology. 2006; 13:933–9. [PubMed: 16788754]
7. Young A, Lyons J, Miller AL, Phan VT, Alarcon IR, McCormick F. Ras signaling and therapies. Adv Cancer Res. 2009; 102:1–17. [PubMed: 19595305]
8. Repasky GA, Chenette EJ, Der CJ. Renewing the conspiracy theory debate: does Raf function alone to mediate Ras oncogenesis? Trends Cell Biol. 2004; 14:639–47. [PubMed: 15519853]
9. Moore MJ, Goldstein D, Hamm J, Figer A, Hecht JR, Gallinger S, et al. Erlotinib plus gemcitabine compared with gemcitabine alone in patients with advanced pancreatic cancer: a phase III trial of the National Cancer Institute of Canada Clinical Trials Group. J Clin Oncol. 2007; 25:1960–6. [PubMed: 17452677]
10. Rinehart J, Adjei AA, Lorusso PM, Waterhouse D, Hecht JR, Natale RB, et al. Multicenter phase II study of the oral MEK inhibitor, CI-1040, in patients with advanced non-small-cell lung, breast, colon, and pancreatic cancer. J Clin Oncol. 2004; 22:4456–62. [PubMed: 15483017]
11. Patnaik, A.; LoRusso, P.; Tabernero, JA.; Laird, D.; Aggarwal, S.; Papadopoulos, K. Biomarker development for XL765, a potent and selective oral dual inhibitor of PI3K and mTOR currently being administered to patients in a Phase I clinical trial. Molecular Targets and Cancer Therapeutics Conference; 2007; San Francisco. p. B265
12. Collisson EA, Sadanandam A, Olson P, Gibb WJ, Truitt M, Gu S, et al. Subtypes of pancreatic ductal adenocarcinoma and their differing responses to therapy. Nature medicine. 2011; 17:500–3.
13. Sun SY, Rosenberg LM, Wang X, Zhou Z, Yue P, Fu H, et al. Activation of Akt and eIF4E survival pathways by rapamycin-mediated mammalian target of rapamycin inhibition. Cancer research. 2005; 65:7052–8. [PubMed: 16103051]
14. O'Reilly KE, Rojo F, She QB, Solit D, Mills GB, Smith D, et al. mTOR inhibition induces upstream receptor tyrosine kinase signaling and activates Akt. Cancer research. 2006; 66:1500–8. [PubMed: 16452206]
15. Mirzoeva OK, Das D, Heiser LM, Bhattacharya S, Siwak D, Gendelman R, et al. Basal subtype and MAPK/ERK kinase (MEK)-phosphoinositide 3-kinase feedback signaling determine susceptibility of breast cancer cells to MEK inhibition. Cancer research. 2009; 69:565–72. [PubMed: 19147570]
16. Jimeno A, Rubio-Viqueira B, Amador ML, Grunwald V, Maitra A, Iacobuzio-Donahue C, et al. Dual mitogen-activated protein kinase and epidermal growth factor receptor inhibition in biliary and pancreatic cancer. Molecular cancer therapeutics. 2007; 6:1079–88. [PubMed: 17363501]
17. Diep CH, Munoz RM, Choudhary A, Von Hoff DD, Han H. Synergistic effect between erlotinib and MEK inhibitors in KRAS wild-type human pancreatic cancer cells. Clinical cancer research : an official journal of the American Association for Cancer Research. 2011; 17:2744–56. [PubMed: 21385921]

18. Gysin S, Rickert P, Kastury K, McMahon M. Analysis of genomic DNA alterations and mRNA expression patterns in a panel of human pancreatic cancer cell lines. Genes Chromosomes Cancer. 2005; 44:37–51. [PubMed: 15929091]
19. Collisson EA, Sadanandam A, Olson P, Gibb WJ, Truitt M, Gu S, et al. Subtypes of pancreatic ductal adenocarcinoma and their differing responses to therapy. Nat Med. 2011; 17:500–3. [PubMed: 21460848]
20. Chou TC, Talalay P. Quantitative analysis of dose-effect relationships: the combined effects of multiple drugs or enzyme inhibitors. Adv Enzyme Regul. 1984; 22:27–55. [PubMed: 6382953]
21. Smyth, GK. Limma: linear models for microarray data. In: Gentleman, R.; Carey, V.; Dudoit, S.; Irizarry, R.; Huber, W., editors. Bioinformatics and Computational Biology Solutions using R and Bioconductor. New York: Springer; 2005. p. 397-420.
22. Gentleman RC, Carey VJ, Bates DM, Bolstad B, Dettling M, Dudoit S, et al. Bioconductor: open software development for computational biology and bioinformatics. Genome Biol. 2004; 5:R80. [PubMed: 15461798]
23. Dabney A, Storey JD, Warnes RD. qvalue: Q-value estimation for false discovery rate control. R package version 12202010.
24. Hastie T, Tibshirani R, Narasimhan B, Chu G. pamr: Pam: prediction analysis for microarrays. R package version 1502010.
25. Team RDC. R: A language and environment for statistical computing. Vienna, Austria: R Foundation for Statistical Computing; 2010.
26. Burk U, Schubert J, Wellner U, Schmalhofer O, Vincan E, Spaderna S, et al. A reciprocal repression between ZEB1 and members of the miR-200 family promotes EMT and invasion in cancer cells. EMBO Rep. 2008; 9:582–9. [PubMed: 18483486]
27. Gregory PA, Bert AG, Paterson EL, Barry SC, Tsykin A, Farshid G, et al. The miR-200 family and miR-205 regulate epithelial to mesenchymal transition by targeting ZEB1 and SIP1. Nature cell biology. 2008; 10:593–601.
28. Peinado H, Olmeda D, Cano A. Snail, Zeb and bHLH factors in tumour progression: an alliance against the epithelial phenotype? Nature reviews Cancer. 2007; 7:415–28.
29. Bracken CP, Gregory PA, Kolesnikoff N, Bert AG, Wang J, Shannon MF, et al. A double-negative feedback loop between ZEB1-SIP1 and the microRNA-200 family regulates epithelial-mesenchymal transition. Cancer research. 2008; 68:7846–54. [PubMed: 18829540]
30. Lacher MD, Shiina M, Chang P, Keller D, Tiirikainen MI, Korn WM. ZEB1 limits adenoviral infectability by transcriptionally repressing the coxsackie virus and adenovirus receptor. Mol Cancer. 2011; 10:91. [PubMed: 21791114]
31. Flaherty KT, Robert C, Hersey P, Nathan P, Garbe C, Milhem M, et al. Improved survival with MEK inhibition in BRAF-mutated melanoma. The New England journal of medicine. 2012; 367:107–14. [PubMed: 22663011]
32. Collisson EA, Trejo CL, Silva JM, Gu S, Korkola JE, Heiser LM, et al. A Central Role for RAF->MEK->ERK Signaling in the Genesis of Pancreatic Ductal Adenocarcinoma. Cancer Discov. 2012
33. Gysin S, Paquette J, McMahon M. Analysis of mRNA Expression Profiles After MEK1/2 Inhibition Reveals Pathways Involved in Drug Sensitivity. Mol Cancer Res. 2012
34. Garraway LA, Janne PA. Circumventing cancer drug resistance in the era of personalized medicine. Cancer Discov. 2012; 2:214–26. [PubMed: 22585993]
35. Chandarlapaty S, Sawai A, Scaltriti M, Rodrik-Outmezguine V, Grbovic-Huezo O, Serra V, et al. AKT inhibition relieves feedback suppression of receptor tyrosine kinase expression and activity. Cancer cell. 2011; 19:58–71. [PubMed: 21215704]
36. O'Reilly KE, Rojo F, She Q-B, Solit D, Mills GB, Smith D, et al. mTOR Inhibition Induces Upstream Receptor Tyrosine Kinase Signaling and Activates Akt. Cancer research. 2006; 66:1500–8. [PubMed: 16452206]
37. Soltoff SP, Carraway KL 3rd, Prigent SA, Gullick WG, Cantley LC. ErbB3 is involved in activation of phosphatidylinositol 3-kinase by epidermal growth factor. Molecular and cellular biology. 1994; 14:3550–8. [PubMed: 7515147]

38. Sergina NV, Rausch M, Wang D, Blair J, Hann B, Shokat KM, et al. Escape from HER-family tyrosine kinase inhibitor therapy by the kinase-inactive HER3. Nature. 2007; 445:437–41. [PubMed: 17206155]

39. Buck E, Eyzaguirre A, Barr S, Thompson S, Sennello R, Young D, et al. Loss of homotypic cell adhesion by epithelial-mesenchymal transition or mutation limits sensitivity to epidermal growth factor receptor inhibition. Molecular cancer therapeutics. 2007; 6:532–41. [PubMed: 17308052]

40. Thomson S, Buck E, Petti F, Griffin G, Brown E, Ramnarine N, et al. Epithelial to mesenchymal transition is a determinant of sensitivity of non-small-cell lung carcinoma cell lines and xenografts to epidermal growth factor receptor inhibition. Cancer research. 2005; 65:9455–62. [PubMed: 16230409]

41. Bryant JL, Britson J, Balko JM, Willian M, Timmons R, Frolov A, et al. A microRNA gene expression signature predicts response to erlotinib in epithelial cancer cell lines and targets EMT. British journal of cancer. 2012; 106:148–56. [PubMed: 22045191]

42. Witta SE, Dziadziuszko R, Yoshida K, Hedman K, Varella-Garcia M, Bunn PA Jr, et al. ErbB-3 expression is associated with E-cadherin and their coexpression restores response to gefitinib in non-small-cell lung cancer (NSCLC). Ann Oncol. 2009; 20:689–95. [PubMed: 19150934]

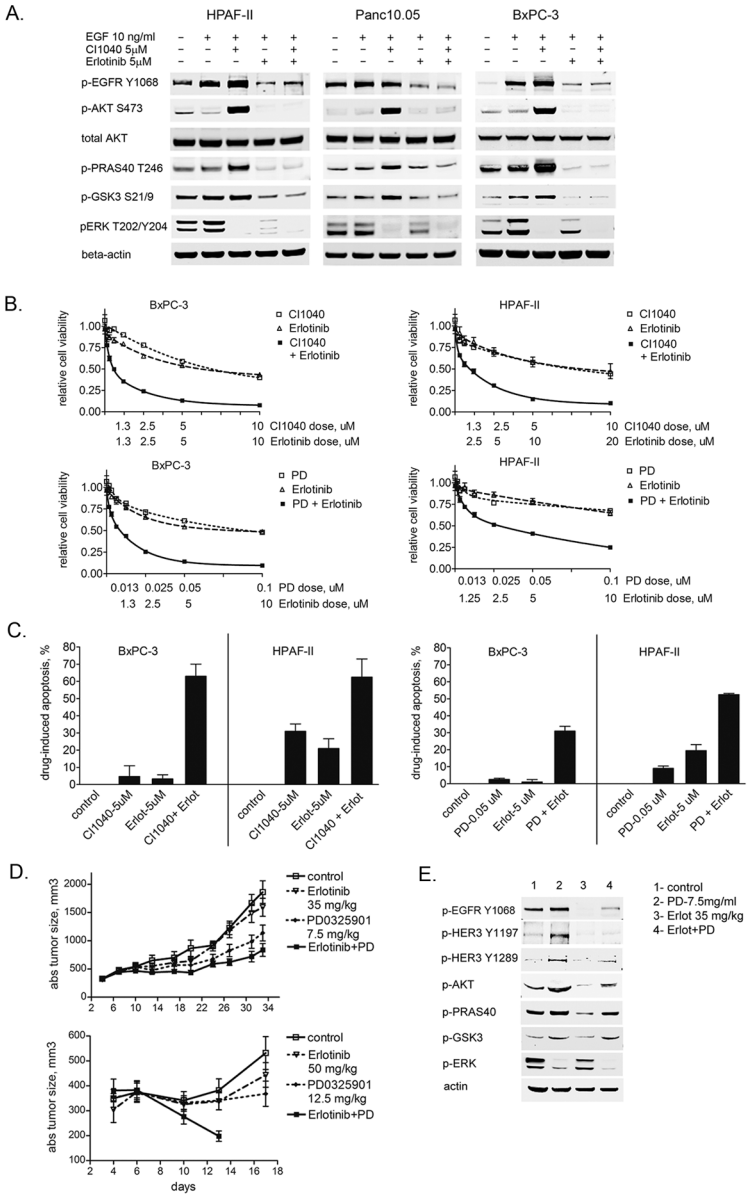

Figure 1.

A. Western blot analysis of the biochemical response of PDAC cell lines treated with the MEK inhibitor CI1040, EGFR inhibitor erlotinib or their combination in low serum conditions (0.1% FBS) stimulated with EGF. Cells were pretreated with the inhibitors for 30 min, treated with EGF and harvested in 4h.

B, C. Synergistic effect of combinations of MEK and EGFR inhibitors on cell growth (B) and apoptosis (C) of pancreatic cancer cell lines. **B:** Dose/effect curves for each inhibitor and their combinations at fixed molar ratio. Cell viability was measured at 72 h after treatment with the drugs. Relative cell viability of drug-treated cells was calculated as a fraction of vehicle treated control. Points, mean of triplicates; bars, SD. **C:** Combination of MEK/EGFR inhibitors results in synergistic induction of apoptosis. Apoptosis was determined by FACS analysis as a total number of annexin V positive cells. Drug-induced apoptosis was calculated by subtraction of apoptosis of control cells from that of drug-treated cells. Columns, mean of duplicates; bars, SD. For each duplicate 40,000 cells were

acquired. The results were confirmed in at least three independent experiments. **D:** Combined inhibition of MEK/EGFR signal transduction pathways inhibits tumor growth *in vivo*. HPAF-II pancreatic cancer xenografts were established in mice. Animals were given PD0325901, Erlotinib, alone or in combination and indicated doses and tumor growth was monitored for 34 days (upper graph) or 18 days at higher doses (lower graph). Eight animals per group were treated and each data point is a mean of eight tumors; bars, SEM. * designates significant difference ($P<0.05$) as determined by ANOVA. **E:** Analysis of target inhibition of EGFR/MEK pathways *in vivo*: tumors of the mice treated by indicated doses of Erlotinib, PD0325901 or their combination were excised and prepared for Western blot analysis on the day 3 of treatment, 3 h post-dosing.

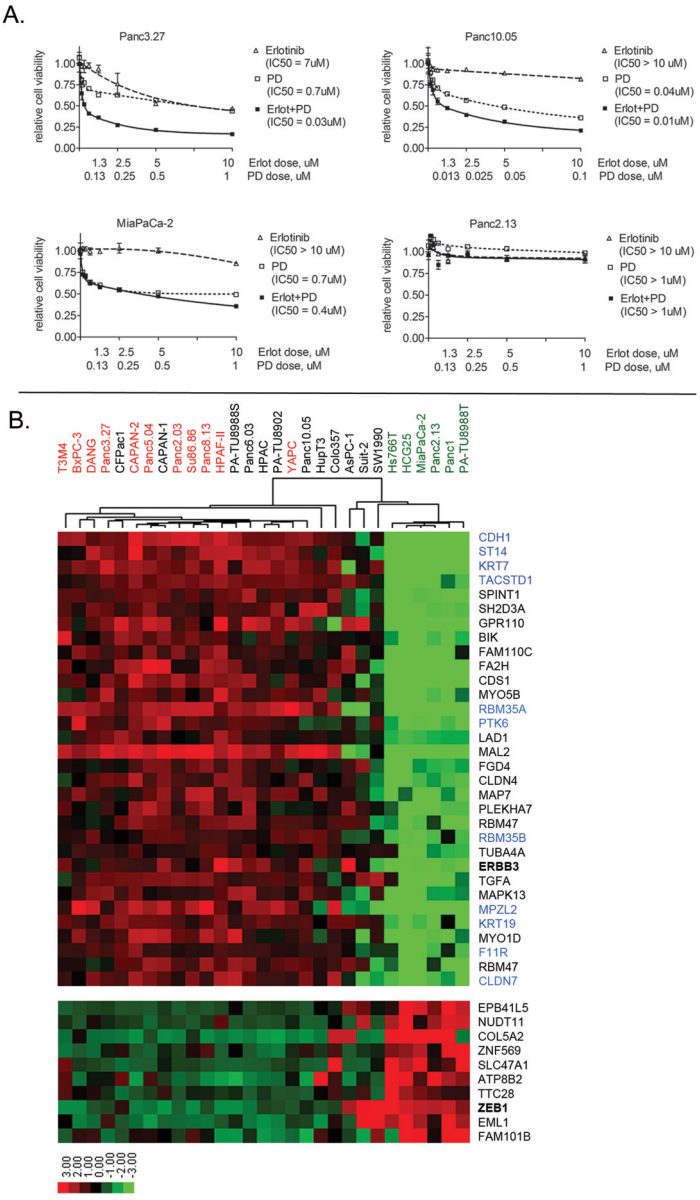

Figure 2.

A: Examples of different responses of pancreatic cell lines to a combination of MEKi PD0325901 and EGFRi erlotinib. Dose/effect curves for each inhibitor and their combinations at fixed molar ratio are presented. IC50 was calculated for each drug and for the combination using GraphPad Prism software. When the combined IC50 was at least 7 fold lower (such as for Panc3.27) or 3-6 fold lower (such as for Panc10.05) than the lowest IC50 of the single agent, the response was classified as strong synergy/potentiation, or as a moderate potentiation, respectively. When the combined IC50 was less than 3 fold different than the lowest IC50 of a single drug, the response was classified as “no combinatorial effect” (as for MiaPaCa-2 or Panc2.13).

B: Results of correlative analysis of predictors of sensitivity (top panel) and resistance (bottom panel) to a combination of PD0325901 and erlotinib. Cell lines were classified by their response as “synergy or moderate potentiation” versus “no combinatorial effect”. This response was correlated with their mRNA expression. The figure illustrates top 32 (q value

< 0.00001, FC > 2.5) and 10 (q value < 0.01, FC > 2.5) predictors of sensitivity and resistance, respectively. Each row represents the relative transcript abundance (in $\log_2$ space) for one gene; each column represents data from one cell line. Within each panel, genes are ordered by *q* value, the most significant predictors are at the top. Cell lines were hierarchically clustered according to their expression of response predictors. Cell line names in red denote those responded with high synergy, the names in black denote those responding with moderate potentiation and the names in green denote those which were resistant to combinatorial effects of MEKi + EGFRi. Gene names shown in blue denote those known to be predominantly expressed in epithelial-type cells.

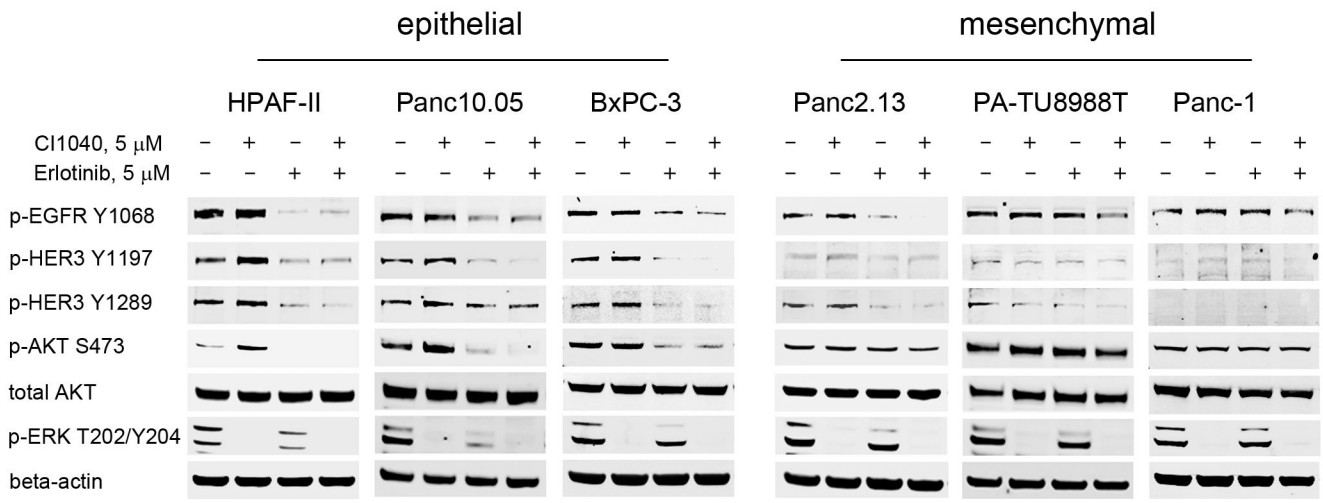

Figure 3.

Western blot analysis of the biochemical response of three epithelial and three mesenchymal PDAC cell lines treated with MEK inhibitor CI1040, EGFR inhibitor erlotinib or their combination. Cells were harvested at 4h after treatment with inhibitors in full serum growth medium. Phospho-Akt levels remain unchanged in response to both inhibitors and their combination in mesenchymal- type compared to epithelial- type cells.

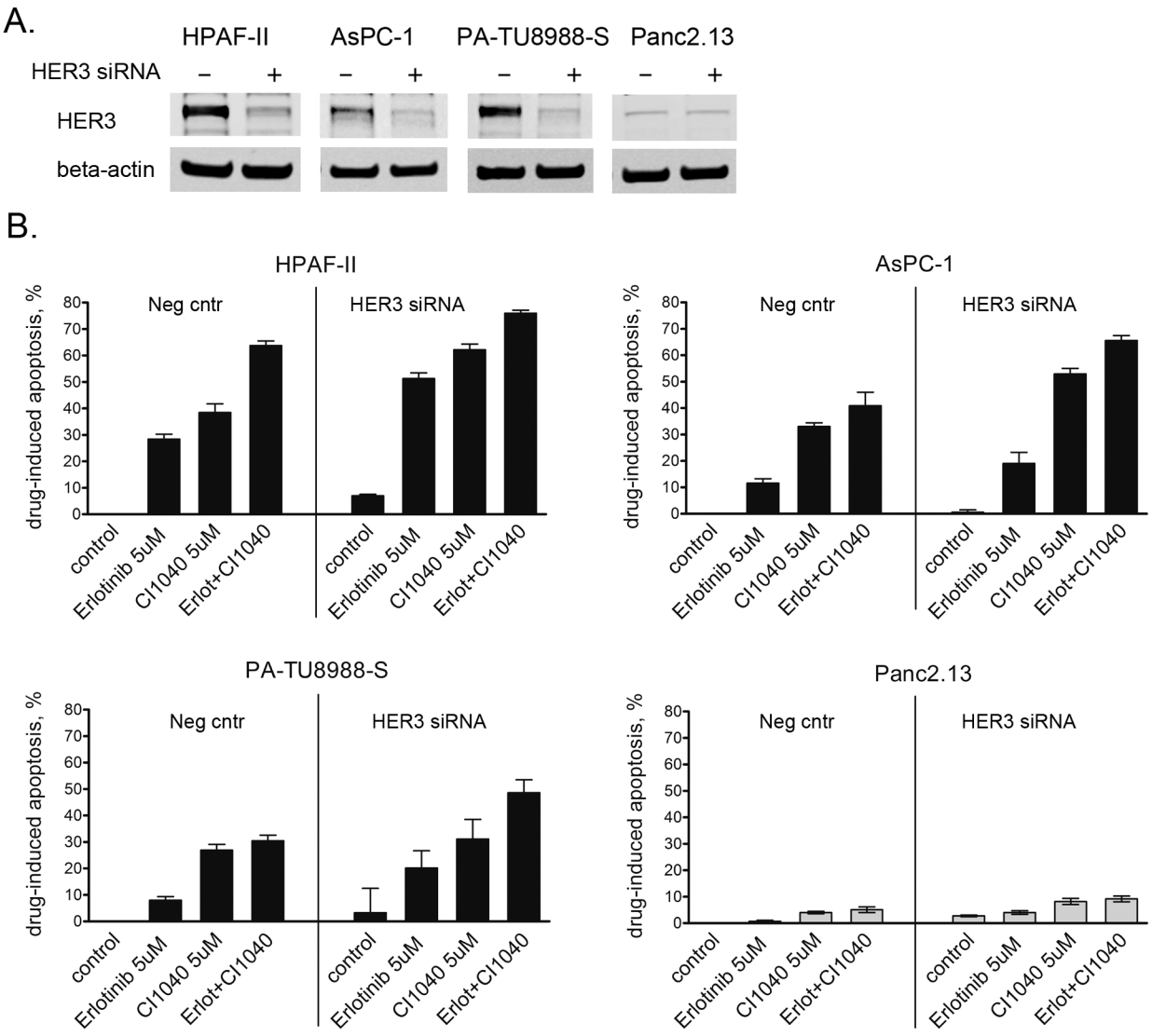

Figure 4.

The effects of HER3 knock-down on epithelial PDAC cell sensitization to MEKi CI1040, EGFRi erlotinib or their combination. **A.** Western blot analysis of HER3 protein expression at 72h post transfection with non-targeting or HER3 siRNA in indicated cell lines. **B**. FACS-based analysis of apoptosis induced by 72h treatment with CI1040, erlotinib or their combination in PDAC cells after prior HER3 knockdown. Cells were treated with the drugs at 72h post HER3 siRNA transfection as described in Materials and Methods. Apoptosis was determined by FACS analysis as a total number of annexin V positive cells. Drug-induced apoptosis was calculated by subtraction of apoptosis of control cells from that of drug-treated cells. Columns, mean of duplicates; bars, SD. For each duplicate, 40,000 cells were acquired. The results were confirmed in at least three independent experiments. Black bars: epithelial subtype, gray bars: mesenchymal subtype cell line.

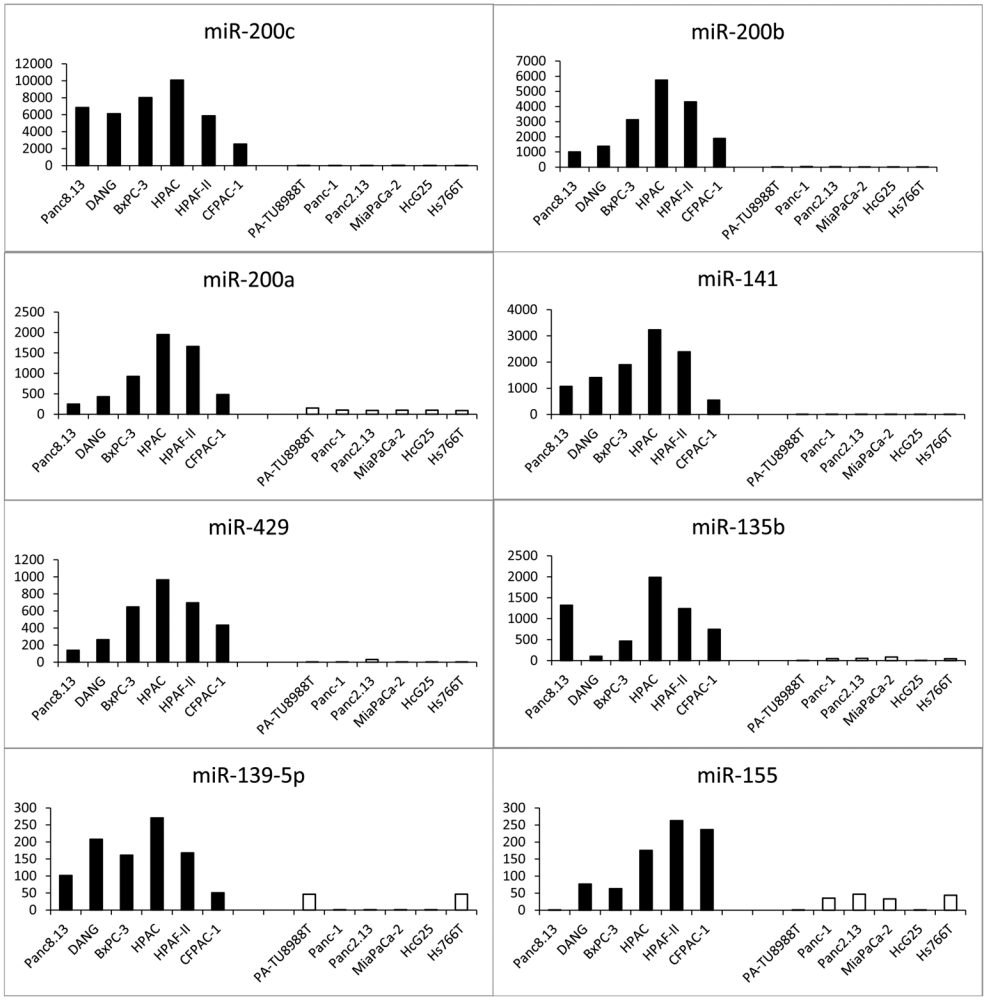

Figure 5.

Relative expression of indicated miRNAs in PDAC cell lines sensitive or resistant to a combination of erlotinib and PD0325901. Direct counts of fluorescent signal as determined by nCounter Assay (Nanostring Tech) are presented. Sensitive cell lines presented by black bars, resistant cell lines are presented by hollow bars.

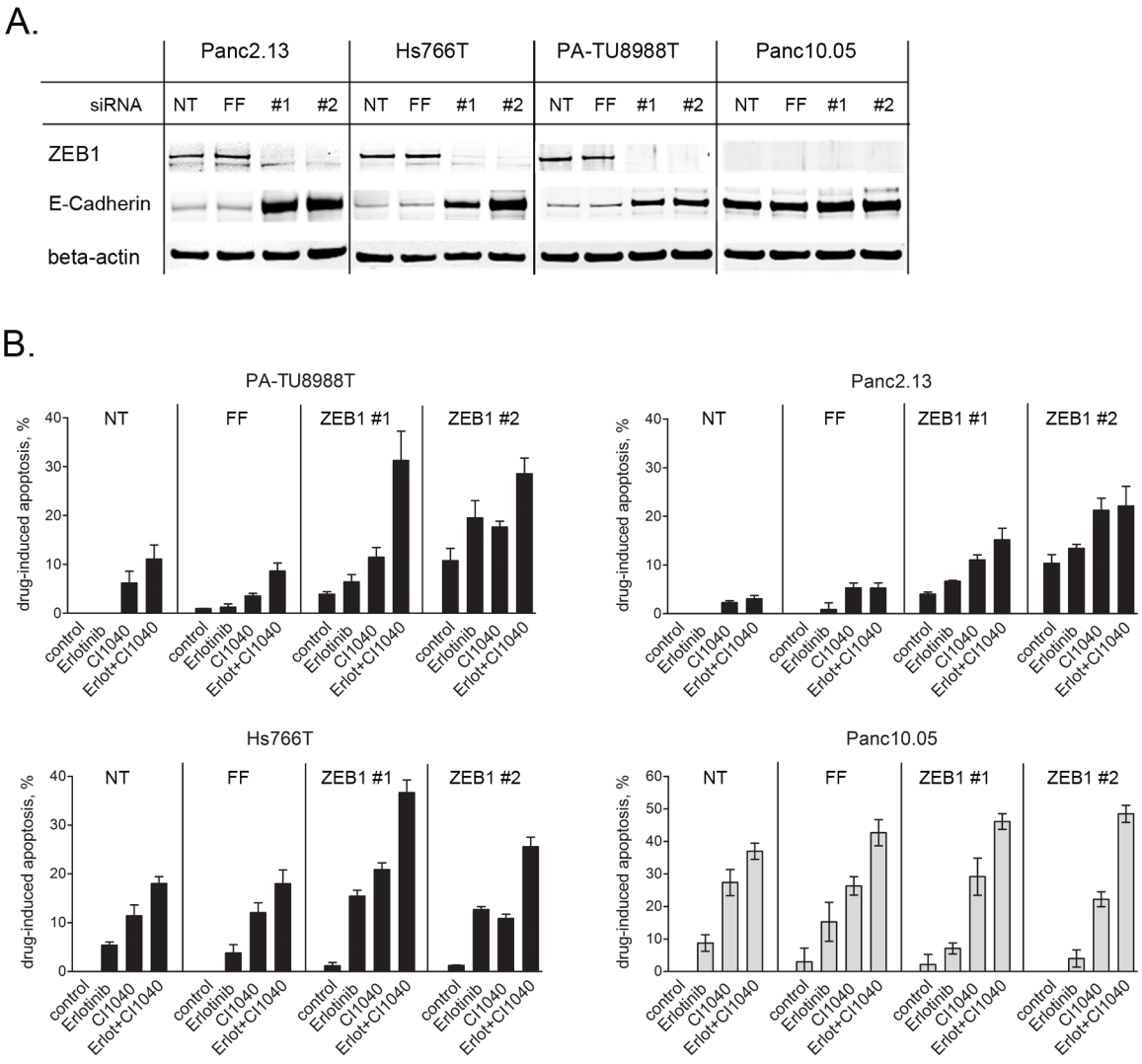

Figure 6.

The effects of ZEB1 knock-down on mesenchymal PDAC cell sensitization to CI1040, erlotinib or their combination. **A.** Western blot analysis of ZEB1 and E-cadherin protein expression at 72h post transfection with two negative controls: non-targeting (NT) and Firefly luciferase targeting (FF) siRNAs and two different ZEB1-targeting siRNAs (ZEB1 #1 and #2). Mesenchymal cell lines expressing ZEB1 protein show significant increase in E-cadherin following ZEB1 knock-down. In contrast, epithelial cell lines express very low amount of ZEB1 and do not show any change post siRNA transfection. **B.** FACS-based analysis of apoptosis induced by 72h treatment with CI1040, erlotinib or their combination in PDAC cells after prior ZEB1 knockdown. Cells were treated with the drugs at 72h post ZEB1 siRNA transfection as described in Materials and Methods. Apoptosis was determined by FACS analysis as a total number of annexin V positive cells. Drug-induced apoptosis was calculated by subtraction of apoptosis of control cells from that of drug-treated cells. Columns, mean of duplicates; bars, SD. For each duplicate, 40,000 cells were acquired. The results were confirmed in at least three independent experiments. Black bars - mesenchymal cell lines, gray bars – epithelial cell line.